J Infrared Milli Terahz Waves (2016) 37:551–560
DOI 10.1007/s10762-015-0240-y

Hysteresis and Frequency Tunability of Gyrotrons

O. Dumbrajs [1,2] · **E. M. Khutoryan** [2,3] · **T. Idehara** [2]

Received: 23 September 2015 / Accepted: 21 December 2015 /
Published online: 9 January 2016

Abstract We present the first devoted theoretical and experimental study of the hysteresis phenomenon in relation to frequency tunability of gyrotrons. In addition, we generalize the theory describing electron tuning of frequency in gyrotrons developed earlier to arbitrary harmonics. It is found that theoretical magnetic and voltage hysteresis loops are about two times larger than experimental loops. In gyrotrons whose cavities have high quality factors, hysteresis allows one only little to broaden the frequency tunability range.

Keywords Gyrotron · Higher harmonics · DNP · NMR · Frequency tunability · Dielectric susceptibility

1 Introduction

In gyrotrons, hysteresis is the phenomenon that causes the amplitude of oscillations to lag behind the magnetic field and the voltage, so that operation regions of modes for rising and falling magnetic field and voltage are not the same. It is intimately linked to existence of the hard excitation region, where for certain parameter values of the gyrotron, stable oscillations can be induced only by kicking the oscillator with the amplitude that is larger than a certain threshold value. Hysteresis-like effects in gyrotron oscillators and their effect mode competition have been studied in [1–3]. In recent years, great interest has developed in the applications of gyrotrons to the enhancement of NMR spectroscopy in the process known as dynamic nuclear

✉ O. Dumbrajs
Olgerts.Dumbrajs@lu.lv

[1] The Institute of Solid State Physics, University of Latvia, Riga LV-1063, Latvia

[2] Research Center for Development of Far-Infrared Region, University of Fukui (FIR UF), Bunkyo 3-9-1, Fukui-shi, Fukui-ken 910-8507, Japan

[3] O.Ya. Usikov Institute for Radiophysics and Electronics of National Academy of Science of Ukraine, 12 ac. Proskura St., Kharkov 61085, Ukraine

polarization (DNP) (see review [4]). In these applications, in contrast to fusion, low-power and low-mode tunable gyrotrons are used. Tuning is achieved by varying the magnetic field or accelerating the voltage so that the operating mode acquires higher axial indices. The low-power and low-mode gyrotrons are especially suitable for studying hysteresis phenomena, because they can oscillate in well-separated low-order modes that allow one to study hysteresis without taking into account the radial mode competition.

2 Fukui 460 GHz Gyrotron FU CW GO-II

At FIR UF, several gyrotrons have been developed for studying high frequency DNP-NMR spectroscopy (see, for example [5, 6]). In this paper, we study the hysteresis phenomenon in the gyrotron FU CW GO-II. Design parameters of this gyrotron are presented in Table 1.

$f_{\mathrm{cut-off}} = 460.231$ GHz. Quality factors of the employed cavity are very high: $Q_{\mathrm{diff}} = 53857$ ($q = 1$), $Q_{\mathrm{ohm}} = 23204$, $Q_{\mathrm{tot}} = 16217$. q is the axial index. For $q = 1$, $f_{\mathrm{cold}} = 460.325$ GHz.

3 Calculations

Theoretically, hysteresis can be studied most conveniently using the time-dependent equation for the oscillation amplitude [1–3]. In such calculations, the equation is solved for a given fixed value of the parameter of interest (magnetic field, accelerating, or modulation voltage) until the onset of stationary oscillations. After this, the parameter is increased by a small amount and calculations are continued until again the onset of stationary calculations. This is repeated until the desired parameter value is reached. Next, such calculations are carried out in the reverse direction with decreasing parameter values.

Table 1 Design parameters of the FU CW GO-II gyrotron

Frequency	459–461 GHz
Frequency tunability	1.5 GHz
Output power	>20 W
Beam energy	20 keV
Pitch factor	1.2
Cavity diameter	5.098 mm
Cavity length	20 mm
Cavity mode	$TE_{8,5}$, second harmonic
Magnet type	10 T SC magnet
Intensity at cavity	8.55 T
Electron gun	Triode MIG
Intensity at gun	0.2 T
Operation mode	CW and pulsed
Beam radius	0.781 mm

3.1 Hysteresis with Respect to Magnetic Field

In Figs. 1, 2, and 3, we show some results of calculations of hysteresis with respect to the magnetic field.

Hence, a large hysteresis region is observed between 8.455 T and 8.483 T. It is interesting to analyze the field profiles at different values of the magnetic field shown in Fig. 2a, b.

At 8.49 T, the field profile has one large peak ($q=1$), efficiency is high. At 8.535 T, the field profile still has one peak ($q=1$), but it is smaller and efficiency is low. At 8.56 T, the field profile has two peaks ($q=2$) and efficiency becomes larger; at 8.57 T, the field profile has three peaks ($q=3$), efficiency still grows. Finally, at 8.585 T, the field profile has four small peaks ($q=4$) and efficiency is negligible.

At 8.57 T, there are three small peaks ($q=3$) and efficiency is noticeable. At 8.54 T, the field profile has one small peak ($q=1$) and efficiency is small. At 8.48 T, the field profile has one large peak ($q=1$) and efficiency is large. At 8.458 T, the peak becomes smaller ($q=1$) and efficiency sharply decreases.

In Fig. 3, frequency tunability due to variation of magnetic field is shown.

It is obvious that the largest tuning range is observed in the region where the field profile acquires the second ($q=2$) and the third maximum ($q=3$). Unfortunately, efficiency in this region is low.

3.2 Hysteresis with Respect to Accelerating Voltage

In Figs. 4 and 5, the results of calculations of hysteresis with respect to accelerating voltage are shown.

It is seen that a large hysteresis region exists between 20 and 22 kV. In Fig. 5, the dependence of frequency and efficiency on voltage is shown.

Comparing Figs. 4 and 5, one can conclude again that in the region of maximal tuning range (higher axial indices), efficiency is low, while in the region, where $q=1$, efficiency is high, but the tuning range is small.

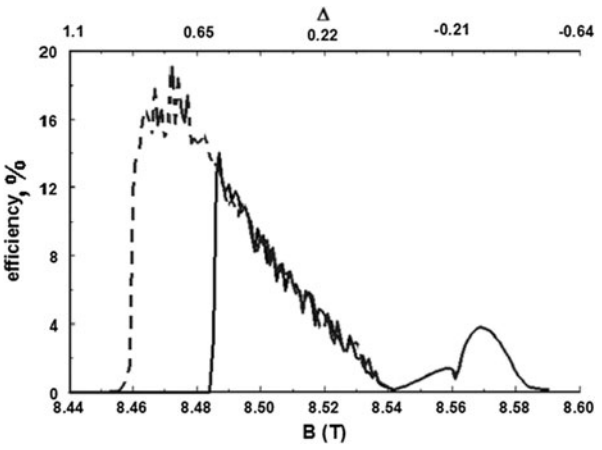

Fig. 1 Efficiency as a function of magnetic field. On the *upper ordinate axis*, frequency mismatch Δ is shown. Calculations were started at 8.44 T and finished at 8.59 T. Oscillation appears at 8.483 T and disappears at 8.59 T (*solid curve*). On the way back, oscillation disappears at 8.455 T (*dashed curve*). Here, $I=0.4$ A and $U=20$ kV

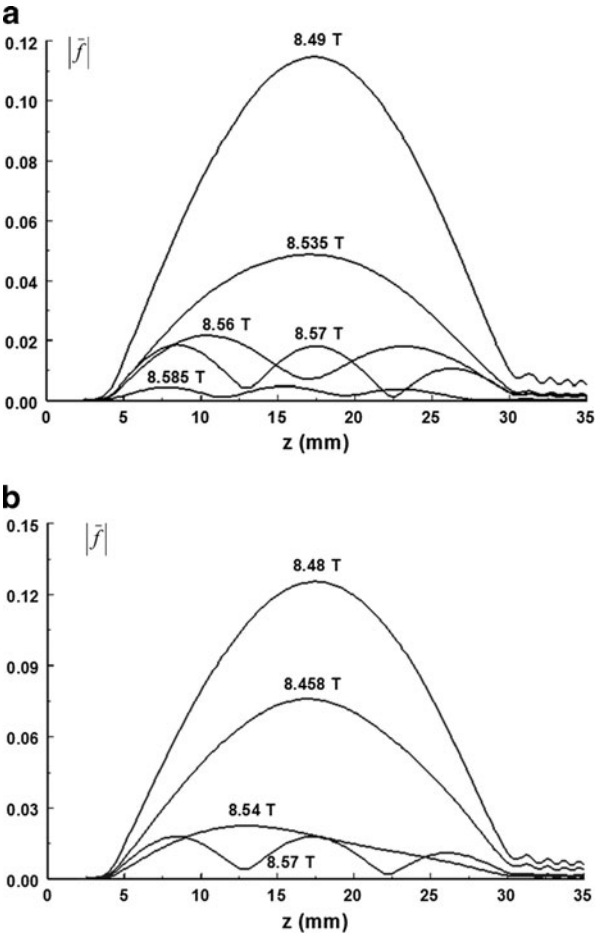

Fig. 2 **a** Field profiles corresponding to increasing magnetic field (*dashed curve* in Fig. 1). **b** Field profiles corresponding to decreasing magnetic field (*dashed curve* in Fig. 1)

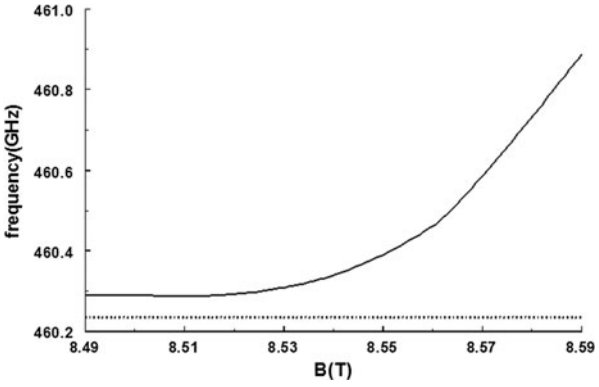

Fig. 3 Frequency as a function of increasing magnetic field. The *dotted horizontal line* marks the cut-off frequency. Here, $I = 0.4$ A

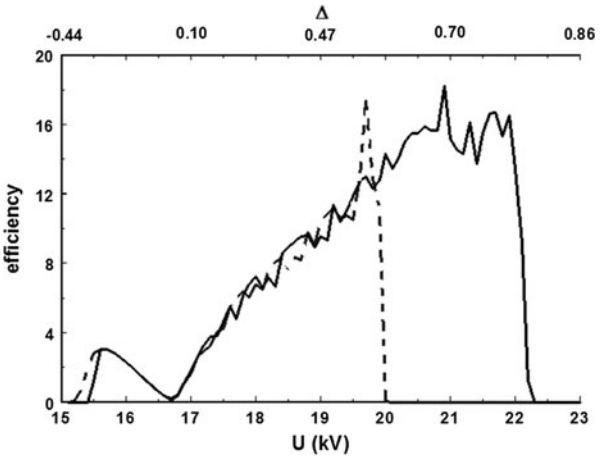

Fig. 4 Calculations were started at 23 kV. When the voltage decreases, oscillations appear at 20 kV and disappear at 15. kV (*dashed curve*). On the way back (*solid curve*),oscillations disappear at 22.3 kV. The *upper ordinate axis* shows the frequency mismatch Δ

4 Experiment

Recently, two second harmonic 460 GHz gyrotrons were designed for DNP-NMR spectroscopy [5, 6]. The length of the middle section of the cavity of the gyrotron named GO-I is 15 mm. This gyrotron was used in the frequency modulation experiments [6]. The length of the middle section of the cavity of the gyrotron named GO-II is 20 mm. This gyrotron was used in the frequency tuning experiments. In Fig. 6, we show experimental results of hysteresis with respect to variation of magnetic field and accelerating voltage for GO-II. The hysteresis loops are ~0.01 T and ~0.3 kV, respectively.

The irregularities of curves below 19 kV in the figure (right) apparently are caused by experimental conditions related to cavity deformation. With decreasing voltage, the output power decreases, but the resonator temperature lags behind. The results shown in this figure should be interpreted so that hysteresis is observed only at high voltages. This is consistent with the theoretical predictions shown in Fig. 4.

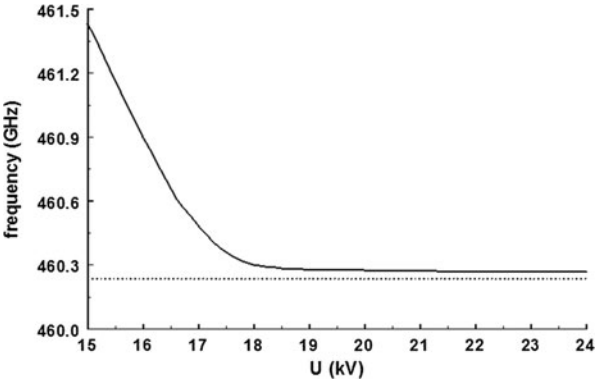

Fig. 5 Frequency as a function of voltage. Here, $B = 8.485$ T

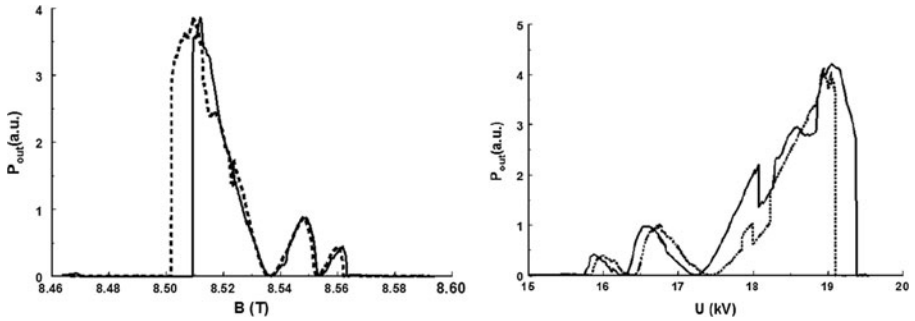

Fig. 6 *Left*: dependence of power on magnetic field. Acceleration voltage 19 kV and current 0.3 A are constant. *Solid and dashed curves* correspond to increasing and decreasing magnetic field, respectively. *Right*: dependence of power on acceleration voltage. Magnetic field $B = 8.51$ T and current 0.3 A are constant. *Solid and dashed curves* correspond to increasing and decreasing voltage, respectively

In Fig. 7, the dependence of frequency and power on the magnetic field is shown.

It can be seen that the experimental results confirm the theoretical predictions: power is low in the region of maximal tuning range and high in the region of small tuning range.

In Fig. 8, we show experimental results of hysteresis with respect to variation of accelerating voltage for GO-I.

One can see that in this case, the hysteresis loop is ~0.4 kV and the frequency tuning range is about 30 MHz wider for the case of increasing voltage. The tuning range for fundamental mode with sufficient power is less than 80 MHz, so the frequency hysteresis is almost half of it. Therefore, for wide frequency modulation range, the modulation voltage waveform should be chosen, taking into account the hysteresis phenomena.

Despite the fact that the theoretical hysteresis loops are significantly larger than the experimental loops, the conclusion can be drawn that a good qualitative agreement between theory and experiment is observed. In the considered gyrotron, a triode gun is used. In these guns, the pitch factor is a rather complicated function of the gun parameters which complicates theoretical calculations. For this reason, the comparison between experiment and theory should be regarded as qualitative. It should also be mentioned that experiments were performed with slightly different values of the operating parameters (magnetic field and voltage) than employed in calculations.

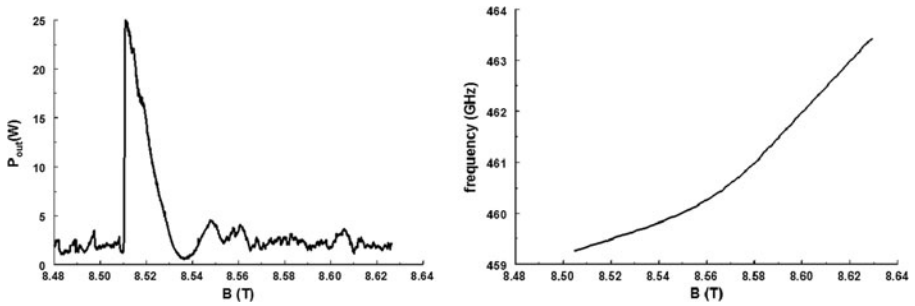

Fig. 7 Dependence of power (*left*) and frequency (*right*) on magnetic field

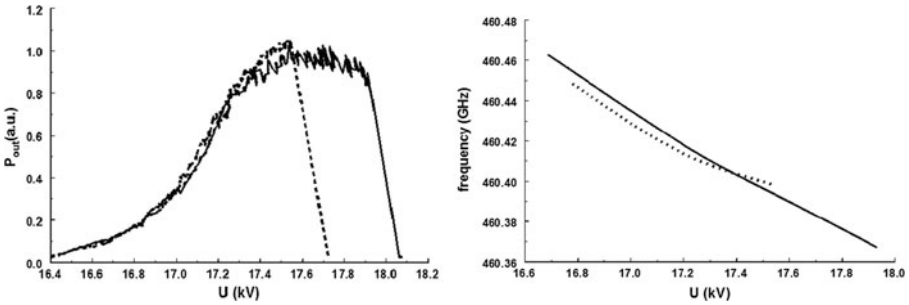

Fig. 8 *Left:* dependence of power on acceleration voltage. Magnetic field $B = 8.51$ T and current 0.17 A are constant. *Solid and dashed curves* correspond to increasing and decreasing voltage, respectively. *Right*: frequency as a function of accelerating voltage

5 Summary

Good qualitative agreement between theory and experiment has been demonstrated. In order to improve the agreement, first of all experimental conditions should be improved: cavity deformation during the voltage change should be avoided and operating parameters should be stabilized. On the theory, side electron velocity spread on hysteresis should be studied.

Unfortunately, in the case of cavities with large quality factors (see Eq. (1)), the hysteresis phenomenon hardly offers a possibility to extend the tuning range of a gyrotron. This might be different in fusion gyrotrons which employ cavities with much lower quality factors (on the order of 1000).

Acknowledgments This work is supported by the Grants in Aid for Scientific Research (B) (No. 24360142) and for Challenging Exploratory Research (No. 25630134) from the Japan Society for Promotion of Science (JSPS) and SENTAN project of JST. This work was performed under the Cooperative Research Programs of the Institute for Protein Research, Osaka University and Research Center for Development of Far Infrared Region, University of Fukui (FIR UF).

Appendix

Electron Tuning of Frequency

To estimate the role of hysteresis in frequency tunability, we use the formalism of electron tuning of frequency developed in [7], generalizing it at the same time to arbitrary harmonics. According to this formalism, for a constant operating current, the frequency shift due to change of electron beam parameters is given by the expression

$$\frac{\delta f}{f} = \frac{1}{2Q_{tot}} \cdot \frac{\partial \kappa}{\partial \Delta} \cdot \delta \Delta \tag{1}$$

where

$$\kappa = -\frac{\mathrm{Re}(\chi)}{\mathrm{Im}(\chi)} \tag{2}$$

The dielectric susceptibility of the electron beam χ is given by the expression

$$\chi = \frac{1}{\pi F}\int_0^{2\pi}\left[\int_0^{\zeta_{out}} p^n(\zeta,\vartheta)\overline{f}^*(\zeta)d\zeta\right]d\vartheta_0 \tag{3}$$

The imaginary part of susceptibility is normalized as follows:

$$\mathrm{Im}(\chi) = \frac{1}{I} \tag{4}$$

where I is the dimensionless current

$$I = 0.238\cdot 10^{-3} I_A Q_{tot}\frac{J_{m\pm n}^2\left(\frac{\nu R_b}{R_{cav}}\right)}{(\nu^2-m^2)J_m^2(\nu)}\cdot\frac{\lambda}{L}\left(\frac{n^n}{2^n n!}\right)\frac{\beta_\perp^{2(n-3)}}{\gamma_{rel}} \tag{5}$$

Here, I_A is the current in amperes, m is the azimuthal index of the mode, n is the harmonic number, ν is the eigenvalue of the mode, R_b is the electron beam radius, R_{cav} is the cavity radius, λ is the wave length, L is the cavity length, $\beta_\perp$ is the normalized perpendicular velocity, and γ_{rel} is the relativistic factor.

The normalized electron perpendicular momentum p can be found by solving the following differential equation:

$$\frac{dp}{d\zeta} + \frac{i}{n}p\left(\Delta + |p|^2 - 1\right) = \overline{if}\left(p^*\right)^{n-1}F, \tag{6}$$

where

$$\zeta = \left(\beta_\perp^2\omega_{cyc}/2\beta_{||}c\right)z \tag{7}$$

is the dimensionless longitudinal coordinate

$$\Delta = \frac{2}{\beta_\perp^2}\left(\frac{\omega_r - n\omega_{cyc}}{\omega_r}\right) \tag{8}$$

is the frequency mismatch. The dimensionless amplitude of stationary oscillations F is given by the expression

$$F = \left(0.47\cdot 10^{-3}\cdot Q_{tot}\cdot P_{out}\frac{J_{m\pm n}^2\left(\frac{\nu}{R_{cav}}\cdot R_b\right)}{\gamma_{rel}U\eta_{el}\beta_{||}\beta_\perp^{2(2-n)}(\nu^2-m^2)J_m^2(\nu)\int_0^{\zeta_{out}}\left|\overline{f}(\zeta)\right|^2 d\zeta}\right)^{\frac{1}{2}}\cdot\left(\frac{n^{n+1/2}}{2^n n!}\right) \tag{9}$$

where P_{out} is the output power, U is the voltage, $\eta_{el} = 1/\left(1 + \left(\frac{\beta_{||}}{\beta_{\perp}}\right)^2\right)$. The field profile $\overline{f}(\zeta)$ which enters into Eqs. (6) and (8) can be found by solving the nonuniform string equation

$$\frac{d^2\overline{f}}{d\zeta^2} + \gamma^2\overline{f} = 0 \tag{10}$$

where

$$\gamma = 2\frac{\beta_{||}}{\beta_{\perp}^2}\frac{c}{\omega}\sqrt{\frac{\omega^2}{c^2} - \frac{\nu^2}{R^2}} \tag{11}$$

Equation (6) has to be suplemented by the initial condition

$$p(\zeta_{in}) = \exp\left(i\frac{\vartheta_0}{n}\right) \qquad (0 \le \vartheta_0 < 2\pi) \tag{12}$$

and Eq. (9) by the boundary conditions

$$d\overline{f}/d\zeta_{|\zeta=0} = i\gamma\overline{f} \tag{13}$$

$$d\overline{f}/d\zeta_{|\zeta=\zeta_{out}} = -i\gamma\overline{f} \tag{14}$$

Extension of Tunability Range due to Hysteresis in the Case of Magnetic Tuning

As seen in Fig. 6, the hysteresis loop lies between $B \approx 8.50\,T$ and $B \approx 8.51\,T$. Corresponding values of Δ and κ are given in Table 2.

Thus,

$$\frac{\partial\kappa}{\partial\Delta} = \frac{-0.84 + 0.93}{0.141 - 0.135} = 15$$

Due to hysteresis, the frequency pulling is

$$\delta f = 460.33 \cdot \frac{1}{2 \cdot 16217} \cdot 15 \cdot (0.141 - 0.085) \cdot 1000 = 11.9\,MHz$$

This value is significantly smaller than the theoretical prediction shown in Fig. 3. For example, the increase of magnetic field from 8.58 to 8.59 T increases the frequency by ~140 *MHz*.

Table 2 Δ and κ as a function of magnetic field

B (T)	Δ	κ
8.50	0.141	−0.84
8.501	0.135	−0.93
8.51	0.085	−2.73

Table 3 Δ as a function of voltage

B (T)	U_{cath} (kV)	Δ
8.51	19.0	0.085
8.51	19.3	0.112

Extension of Tunability Range due to Hysteresis in the Case of Voltage Tuning

As seen in Fig. 6, the hysteresis loop lies between $U \approx 19\,\text{kV}$ and $U \approx 19.3\,\text{kV}$. Corresponding values of Δ are given in Table 3.

Due to hysteresis, the frequency pulling is

$$\delta f = 460.33 \cdot \frac{1}{2 \cdot 16217} \cdot 15 \cdot (0.112 - 0.085) \cdot 1000 = 5.7\,\text{MHz}$$

This value also is significantly smaller than the theoretical prediction shown in Fig. 5. For example, the variation of voltage between 15 and 15.3 kV results in frequency variation on the order ~100 MHz.

Triode Gun

In this gyrotron, a triode gun is used with the following parameters: the magnetic compression $b = 43.6$, the distance between the cathode and the anode $d = 3.8\,\text{mm}$, the cathode angle $\theta_c = 39.1°$, and the cathode radius $R_c = 6\,\text{mm}$. Although the electron gun has been carefully designed with the E-Gun code to form a laminar electron beam, the velocity pitch factor is evaluated with an analytic expression in the simulation calculations. The dimensionless perpendicular electron velocity is given by the standard expression:

$$\beta_\perp = \frac{1}{\gamma_{rel} c} \cdot \frac{b^{3/2}}{B} \cdot \frac{(\cos\theta_c)^2}{R_c \ln[1 + (d\cos\theta_c)/R_c]} \cdot U_{\text{mod}} \tag{15}$$

Here, $\gamma_{rel} = 1 + U/511$ B is the magnetic field in the cavity, and U_{mod} is the modulation voltage. In this particular gun, $U_{\text{mod}} = 8.7\,kV$.

References

1. O. Dumbrajs, T. Idehara, Y. Iwata, S Mitsudo, I. Ogawa, B. Piosczyk, Hysteresis-like effects in gyrotron oscillators, Physics of Plasmas 10, 1183-1186 (2003).
2. O. Dumbrajs and T. Idehara, "Hysteresis in mode competition in high power 170 GHz gyrotron for ITER" Int. J. Infrared Milimeter Waves 29, 232 (2008).
3. O. Dumbrajs and G.S. Nusinovich, To the theory of high-power gyrotrons with uptapered resonators, Physics of Plasmas 17, 053104-1-053104-6 (2010).
4. R.J. Temkin, THz gyrotrons and their applications, IRMMW-THz 2014, Tuscon, AZ, USA, Sep. 14-19, 2014.
5. T. Idehara, Y. Tatematsu, Y. Yamaguchi, E.M. Khutoryan, A.N. Kuleshov, K. Ueda, Y. Matsuki, and T. Fujiwara, The development of 460 GHz gyrotrons for MHz DNP-NMR spectroscopy, J. Infrared, Millimeter and Terahertz Waves 36, 613-627 (2015).
6. T. Idehara, E.M. Khutoryan, Y. Tatematsu, Y. Yamaguchi, A.N. Kuleshov, O. Dumbrajs, Y. Matsuki, and T. Fuiwara, High-speed frequency modulation of 460 GHz gyrotron for enhancement of 700 MHz DNP-NMR spectroscopy, J. Infrared, Millimeter and Terahertz Waves 36, 819 - 829 (2015).
7. I.I. Antakov, E.V. Zasypkin, and E.V. Sokolov, Electron tuning of frequency in gyrotrons, Int. J. Infrared Millimeter Waves 14, 1001-1015 (1993).